International Journal of Chemical, Materials and Biomolecular Sciences
ISSN: 2415-6620
Vol:14, No:6, 2020

Ozone Assisted Low Temperature Catalytic Benzene Oxidation over Al_2O_3, SiO_2, AlOOH Supported Ni/Pd Catalytic

V. Georgiev

***Abstract*—**Catalytic oxidation of benzene assisted by ozone, on alumina, silica, and boehmite-supported Ni/Pd catalysts was investigated at 353 K to assess the influence of the support on the reaction. Three bimetallic Ni/Pd nanosized samples with loading 4.7% of Ni and 0.17% of Pd supported on SiO_2, AlOOH and Al_2O_3 were synthesized by the extractive-pyrolytic method. The phase composition was characterized by means of XRD and the surface area and pore size were estimated using Brunauer–Emmett–Teller (BET) and Barrett–Joyner–Halenda (BJH) methods. At the beginning of the reaction, catalysts were significantly deactivated due to the accumulation of intermediates on the catalyst surface and after 60 minutes it turned stable. Ni/Pd/AlOOH catalyst showed the highest steady-state activity in comparison with the $Ni/Pd/SiO_2$ and $Ni/Pd/Al_2O_3$ catalysts. Their activity depends on the ozone decomposition potential of the catalysts because of generating oxidizing active species. The sample with the highest ozone decomposition ability which correlated to the surface area of the support oxidizes benzene to the highest extent.

***Keywords*—**Ozone, catalysts, oxidation, Volatile organic compounds, VOCs.

I. Introduction

MODERN chemical industry involves the use of benzene as a component for the manufacturing of various products such as gasoline and other fuels, glues, paints, furniture wax, adhesives, coating, rubbers and more. According to the Centers for Disease Control and Prevention (CDC) it ranks in the top 20 chemicals for production volume [20]. Along with the useful properties, benzene belongs to the group of hazardous air pollutants (HAPs). Furthermore, it occupies the sixth position in the priority list of hazardous substances of ATSDR (Agency for Toxic Substances and Disease Registry) and has a strong negative impact on the human body [21]. Depending on the various routes of exposure, inhalation, oral or dermal, benzene causes death, systemic, immunological, neurological, reproductive, developmental, genotoxic, and carcinogenic effects. Because of their harmful effects, the need arises for its control in the ground level of the atmosphere mostly. Among the thermal combustion and absorption techniques, catalytic oxidation is a very promising process for the removal of such air pollution [1], [2]. Various catalytic systems suitable for the oxidation of VOCs are available in the literature. There are a number of reports related to using metal oxides as well as noble metals for air pollution removal [22].

Metal oxide catalysts can be sorted into three groups, according to their electrical properties: n-type semiconductors, p-type semiconductors, and insulators. These properties are related to their catalytic behavior. Generally, the n-type metal oxides are not active as oxidation catalysts since they lose oxygen upon heating in contrast to the p-type ones which are considered to be active in oxidation reactions because they gain oxygen.

Insulators have very low electron mobility and are generally not active catalysts. It has been found [23] that the mechanism of oxidation on p-type oxides involves adsorbed 0^-, which leads to more active oxygen species than the n-type oxides involving lattice oxide ions. Such metal oxides are considered to be oxides of V, Cr, Mn, Fe, Co, Ni, and Cu as the TiO_2 supported metal oxide (e.g. Cu, Mn) catalysts, in various loading effectively destroy toluene, benzene and xylene (BTX) without any by-products in the temperature range of 300-350 °C [3], [4].

Supported noble catalysts on the basis of Pt, Pd, Ag, and Au are effectively used in VOCs' complete oxidation [5]-[8]. Frequently these metals are mixed with Ru, Rh, Os, Ir, or Y supported on Al_2O_3, SiO_2 or CeO_2 [4]. Platinum catalysts on alumina or active carbon are successfully applied to control the VOCs concentration with light-off temperatures ranged between 130 and 150°C [9], [10]. Besides the above-mentioned approaches for removal these organic pollutants, ozone assisted oxidation has been reported as a promising energy-saving method. Involving ozone, Einaga and Futamura have carried out catalytic oxidation of cyclohexane and benzene over alumina-supported Mn, Ag, Ni, Co, Fe and Cu oxides at room temperature showing that the manganese catalyst is the most effective among them [11], [12].

The oxidation process includes the formation of intermediate compounds such as alcohols, ketones, a lactone, acid anhydrides and carboxylic acids on the catalyst surface subsequently decomposed by ozone feed. Metals such as Mn, Fe, Ni, Ag, Co supported on TiO_2 and ZSM-5 were utilized for catalytic oxidation of toluene under temperatures below 100 °C [13]. Naydenov and Mehanjiev have investigated the kinetics of complete catalytic oxidation of benzene by ozone on MnOx suggesting that the rate-determining step of complete oxidation by ozone is the ozone decomposition [14], [15]**.** In this process, active oxygen species capable of oxidizing the organic compounds are formed on the metal oxide surface. Despite the success in the destruction of the

V. Georgiev is with the Institute of Catalysis – Bulgarian Academy of Sciences, Sofia 1113, Bulgaria (e-mail: vlado@ic.bas.bg).

toxic air pollution, there is still a need for investigating the more economically and effectively ways for disposal of such substances.

The aim of the present work is to investigate the performance of nickel/palladium supported on SiO_2; Al_2O_3 and AlOOH (boehmite) catalysts, prepared by the extractive-pyrolytic method in benzene oxidation with ozone.

II. Experimental

The extractive-pyrolytic method (EPM) was used for the preparation of the samples. This method allows small amounts of noble metals (1–5%) with particle sizes ranging from several nanometers to tens of nanometers to be attached onto the surface of the support. Its simplicity and low cost characterize the EPM as a promising method for nanosized catalysts synthesis. Nickel and palladium precursors were prepared at first as described in detail elsewhere [16], [17]. As carriers, we used plasma processed nanopowders of Al_2O_3, commercial nanopowders of γ-AlO(OH) and SiO_2 nanopowders. Finally, the carrier samples were dispersed in a solution of the precursor, then it was dried and thermally treated by heating from room temperature until 300 °C and by annealing for 5 min in air. Thus, three bimetallic Ni/Pd nanosized samples with loading 4.7% of Ni and 0.17% of Pd supported on silica, alumina and aluminum hydroxide oxide were synthesized.

X-ray powder diffraction (XRD) measurements were performed using Bruker D8 Advance powder diffractometer employing a Copper Line Focus X-ray tube producing Kα radiation by a generator operating at 45 kV and 40 mA. The data collections were undertaken with the range from 10° to 80° at a rate of 0.04° s^{-1}.

The texture characteristics as BET surface area and pore size were determined at a low temperature of 77 K using Quantachrome Instruments NOVA 1200e analyzer.

The catalytic performance of the samples was tested in a fixed bed continuous flow reactor, under 353 K and atmospheric pressure, connected to a Hewlett Packard 5890 series II gas chromatograph equipped with a flame ionization detector. The experiments were carried out under the following conditions: catalyst bed volume 0.5 cm^3 (particle size 0.25–0.50 mm), inlet benzene concentration 42 g/m^{-3} in air, ozone concentration 10000 ppm and space velocity 4000 h^{-1}. The gas chromatographic analysis was performed using a capillary HP Plot Q column appropriate to separate the products of the eventual mild benzene oxidation. Ozone was prepared by passing oxygen through a 4-9 kV discharge. The ozone concentration in the gas phase at the reactor inlet ($[O_3]_o$) has been measured by BMT 964 ozone analyzer. The experimental scheme is represented in Fig. 1.

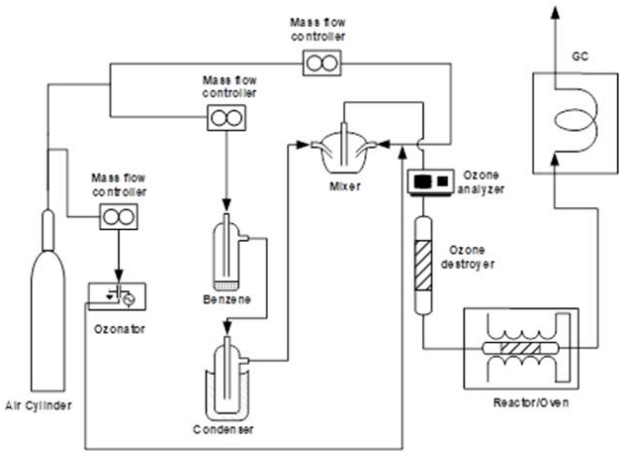

Fig. 1 Schematic diagram of experimental setup

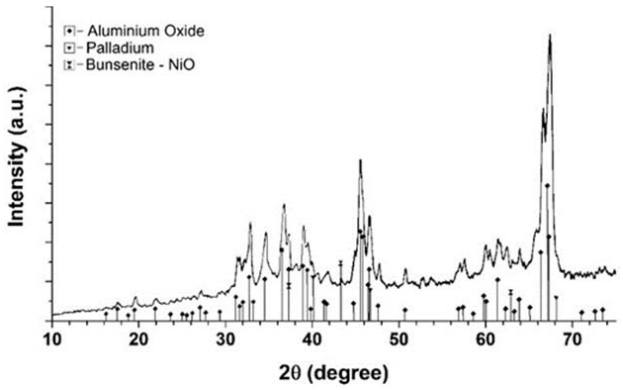

Fig. 2 The XRD patterns of the Ni/Pd/Al_2O_3 catalyst

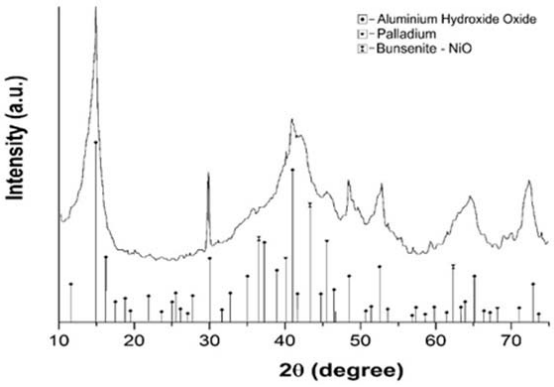

Fig. 3 The XRD patterns of the Ni/Pd/AlO(OH) catalyst

III. Result and Discussion

A. Catalyst Characterization

The crystalline phase composition of prepared catalytic samples was analyzed by XRD. Fig. 2 shows the XRD patterns of Ni/Pd catalysts supported on Al_2O_3.

Fig. 2 shows the spectrum of Ni/Pd/Al_2O_3. The main peaks correspond to a tetragonal Al_2O_3, whose content dominates over that of the Ni and Palladium, which are also represented in the spectrum. Characteristic peaks at 2θ = 40.2, 46.7 and 68.2, which are typical for a metallic Pd phase (JCPDS Card No. 46-1043 face-centered cubic crystal system with a = 3.89019 Å) are found in the spectrum. Distinct peaks at 2θ = 37.06, 43.095, 62.620 that have been identified as peaks of cubic NiO crystallites. The XRD pattern revealed the

formation of a cubic phase of NiO (JCPDS No. 01-071-1179) with a lattice constant, a = 4.1771 Å.

Fig. 3 represents the XRD spectrum of the Ni/Pd/AlO(OH) catalyst. The majority of the peaks are assigned to AlO(OH). The diffraction pattern indicates peaks characteristic for Pd and NiO appearing at the same degrees as on the spectrum in Fig. 2.

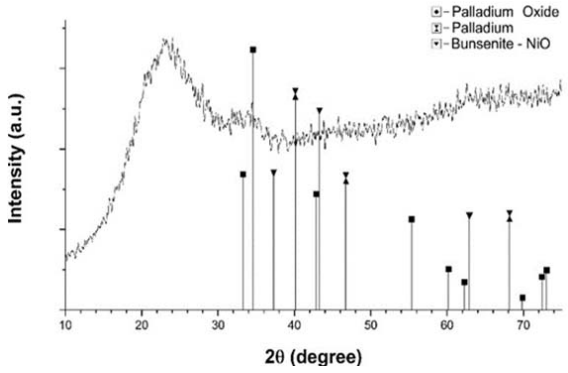

Fig. 4 The XRD patterns of the Ni/Pd/Al_2O_3 catalyst

A very broad signal around 25° 2theta attributed to amorphous silica can be seen on the spectrum of Ni/Pd/SiO_2 (Fig. 4). Such broadening of peaks is typical for materials in which diffraction does not occur due to the absence of a regular crystal structure with planes where refraction can take place. A possible explanation of appearing this peak is the existence of short-range order i.e. fixed distance between bonds in the amorphous material, obviously in our case the Si-O bond.

TABLE I
SPECIFIC SURFACE AREA, PORE SIZE AND PORE VOLUME OF THE SAMPLES

Sample	S_{BET} [m^2/g]	V_t [cm^3/g]	D_{av} [nm]
Ni/Pd/SiO_2	126	1.37	19.76
Ni/Pd/Al_2O_3	103	0.82	33.2
Ni/Pd/AlOOH	168	0.44	8.3

All the surface area data and porous characteristics of the samples are summarized and shown in Table I. The highest surface area shows a catalyst supported on silica, which should facilitate the decomposition of ozone to a greater extent than other samples and enhance oxidation of the substrate. Fig. 5 shows the N_2 adsorption-desorption isotherms and BJH desorption pore size distribution analysis of the catalysts. The N_2 adsorption-desorption isotherms of all samples displayed an approximate type IV isotherm as defined by the International Union of Pure and Applied Chemistry (IUPAC). The presence of a type H3 hysteresis loop indicates the existence of mesopores, and the unlimited adsorption at high P/P0 values suggests that aggregates of plate-like particles give rise to slit-shaped pores [18].

Due to the large number of 8.3 nm in size pores, Ni/Pd/AlOOH produces the largest surface area of 168 m^2/g, which is much higher than that of the other catalysts. The lowest SBET exhibits the sample of Ni/Pd/Al_2O_3 with a 103 m^2/g surface area and an average pore diameter of 33.2 nm.

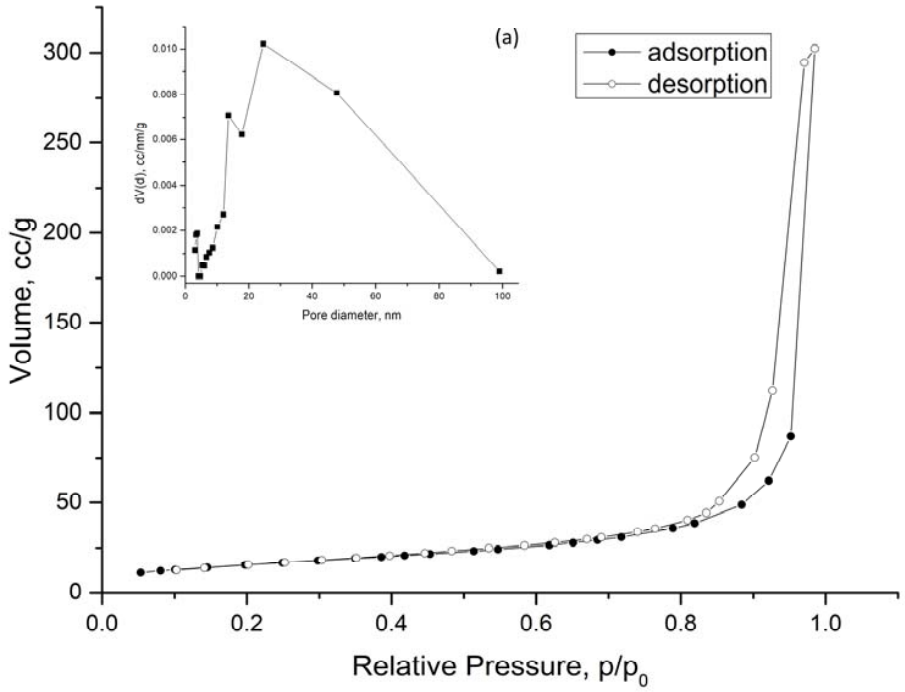

Fig. 5 (a) N2 adsorption-desorption isotherms and the BJH desorption pore size distribution for the Ni/Pd/Al_2O_3

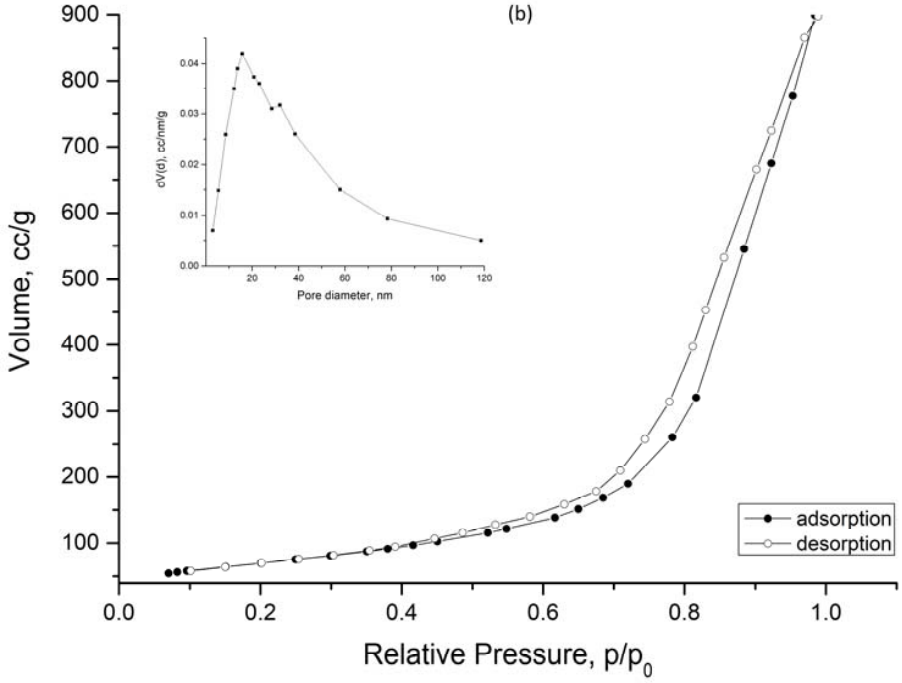

Fig. 5 (b) N_2 adsorption-desorption isotherms and the BJH desorption pore size distribution for the Ni/Pd/SiO_2

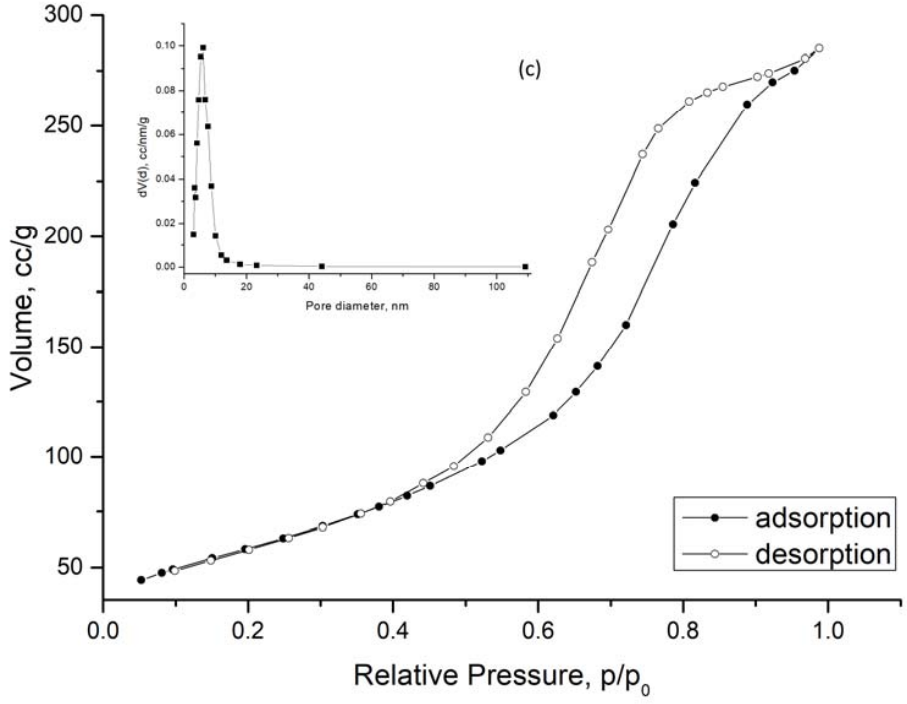

Fig. 5 (c) N2 adsorption-desorption isotherms and the BJH desorption pore size distribution for the Ni/Pd/AlOOH.

B. Catalytic Activity Tests

Fig. 6 shows the catalytic activity of the catalysts with respect to the oxidation of benzene assisted by ozone. The course profiles for benzene oxidation over samples tested show lowering the benzene oxidation with time. The decrease in the conversion of benzene can be explained by the accumulation of intermediates in the process of decomposition of benzene, which cover the surface of the catalyst and thus block the active sites and inhibit the oxidation.

A steady-state conversion was achieved for all samples after

60 minutes. It was expected that the amorphous silica having a disordered surface with more surface defects to interact with organics will be most active in benzene oxidation, but the highest activity was observed for Ni/Pd/Boehmite with above 60% conversion in the steady-state part of the test. The lowest activity was registered for the sample supported on alumina showing about 30% conversion. The catalyst surface area, which is one of the important factors for obtaining a high catalytic reaction rate, differs to some extent for each sample. From Table I, it can be seen that the sample surface area reflected on the benzene oxidation rate and the Ni/Pd/AlOOH catalyst with the highest BET area exhibited the highest activity.

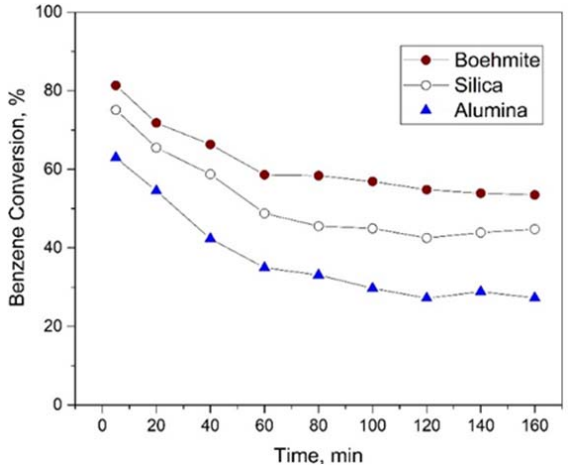

Fig. 6 Time course for benzene oxidation with ozone over Ni/Pd catalysts supported on Boehmite, Silica, and Alumina

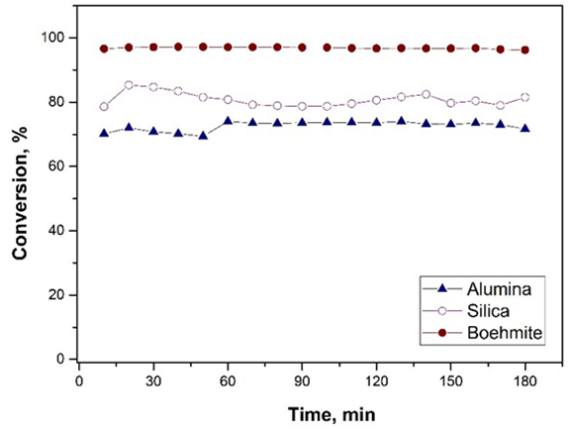

Fig. 7 Ozone conversion as a function of ozonation time for the Ni/Pd catalytic samples (the supports are denoted in the graph legend)

In order to explain the influence of the support on the activity of the catalysts in terms of the benzene oxidation, the ozone decomposition on tested samples should be taken into consideration. The catalytic activity of the supported Ni/Pd catalysts in ozone decomposition was measured by monitoring the inlet and outlet ozone concentrations and calculating the conversion of ozone to molecular oxygen. It was found that all treated Ni/Pd catalytic samples have activity with respect to the ozone decomposition reaction, but the maximum conversion degree (more than 90%) is observed in the case of boehmite-supported Ni/Pd system (Fig. 7).

Since ozone has low oxidizing ability with regard to aromatic compounds and alkanes, the role of the catalysts is to transform ozone to active oxygen species that can oxidize these compounds. Einaga et al. have explained the mechanism of ozone decomposition over silica-supported manganese catalysts and its role in the benzene oxidation [19]. It was reported that ozone was decomposed on the catalysts according to (1)-(4), to form oxygen species that take part in the oxidation.

$$O_3 + * \rightarrow O_2 + O^* \quad (1)$$

$$O^* + O_3 \rightarrow O_2 + O_2^* \quad (2)$$

$$O_2^* \rightarrow O_2 + * \quad (3)$$

$$O^* + C_6H_6 \rightarrow decomposition \quad (4)$$

* denotes the catalyst active site. Thus, the ability of the catalyst to utilize the ozone molecules plays a critical role in the oxidation of benzene. The catalysts showed stable activity to decompose ozone during the time of the tests and Ni/Pd/AlOOH achieves about 97% conversion which is the highest among the samples. By comparing Figs. 6 and depicting ozone decomposition and the conversion of benzene respectively, it can be seen that the Ni/ Pd/AlOOH catalyst that decomposes ozone to the highest extend is the most effective in the benzene oxidation as well. The efficiency of the catalysts in regard to the reaction decreases in the following order Ni/Pd/AlOOH > Ni/Pd/SiO_2 > Ni/Pd/Al_2O_3.

IV. Conclusion

In this work, we investigated the catalytic activity of boehmite (AlOOH), silica and alumina-supported Ni/Pd catalysts prepared by EPM. Ni/Pd/AlOOH catalyst showed the highest steady-state activity for benzene oxidation with ozone at 343 K, in comparison with the Ni/Pd/SiO_2 and Ni/Pd/Al_2O_3 catalysts. A strong correlation is observed between the conversion extent of benzene and that of ozone. The catalytic activity of the catalysts increased with the increase of the ozone decomposition potential of the samples which was related to the surface area. Thus, the benzene oxidation rate was affected to the highest extent by the surface area of the support.

References

[1] K. Everaert, J. Baeyens, "Catalytic combustion of volatile organic compounds," *Journal of Hazardous Materials*, vol. B, pp. 113-139, 2004.

[2] A. M. Venezia, L. F. Liotta, G. Pantaleo, A. Longo, "Ceria-Based Catalysts for Air Pollution Abatement," *Catalysis by Ceria and Related Materials*, vol. 14, pp. 813-879, 2013.

[3] Kim Sang Chai, "The catalytic oxidation of aromatic hydrocarbons over supported metal oxide," *Journal of Hazardous Materials*, vol. B, № 91, pp. 285–299, 2002.

[4] Spivey, James J, "Complete Catalytic Oxidation of Volatile Organics," *Ind. Eng. Chem. Res*., vol. 26, pp. 2165-2180, 1987.
[5] Wu, H., Pantaleo, G., Venezia, A.M., Liotta, L.F., Mesoporous silica based gold catalysts: Novel synthesis and application in catalytic oxidation of CO and volatile organic compounds (VOCs), *Catalysts*, vol. 3, № 4, pp. 774-793, 2013.
[6] Zahra Abbasi, Mohammad Haghighi, Esmaeil Fatehifar, Saeed Saedy, "Synthesis and physicochemical characterizations of nanostructured Pt/Al2O3–CeO2 catalysts for total oxidation of VOCs," *Journal of Hazardous Materials*, vol. 186, № 2-3, pp. 1445-1454, 2011.
[7] S. Morales-Torres, F.J. Maldonado-Hódar, A.F. Pérez-Cadenas, F. Carrasco-Marín, "Design of low-temperature Pt-carbon combustion catalysts for VOC's treatments," *Journal of Hazardous Materials*, vol. 183, № 1-3, pp. 814-822, 2010.
[8] Liotta, L.F., "Catalytic oxidation of volatile organic compounds on supported noble metals," *Applied Catalysis B: Environmental*, vol. 100, № 3-4, pp. 403-412, 2010.
[9] Jeffrey Chi-Sheng Wu, Zhi-An Lin, Feng-Ming Tsai, Jen-Wei Pan, "Low-temperature complete oxidation of BTX on Pt/activated carbon catalysts," *Catalysis Today*, vol. 63, pp. 419–426, 2000.
[10] Salvador Ordóñez, Lisardo Bello, Herminio Sastre, Roberto Rosal, Fernando V. D´ıez, *Applied Catalysis B: Environmental*, vol. 38, pp. 139–149, 2002.
[11] Hisahiro Einaga, Shigeru Futamura, "Oxidation behavior of cyclohexane on alumina-supported manganese oxides with ozone," *Applied Catalysis B: Environmental*, vol. 60, pp. 49–55, 2005.
[12] H. Einaga, S. Futamura, "Comparative study on the catalytic activities of alumina-supported metal oxides for oxidation of benzene and cyclohexane with ozone," *React. Kinet. Catal. Lett*., vol. 81, pp. 121–128, 2004.
[13] M. Sugasawa, A. Ogata, "Effect of different combination of metal and zeolite on ozone-assisted catalysis for toluene removal," *Ozone: Sci. Eng*., vol. 33, pp. 158–163, 2011.
[14] P. Konova, M. Stoyanova, A. Naydenov, St. Christoskova, D. Mehandjiev, "Catalytic oxidation of VOCs and CO by ozone over alumina supported cobalt oxide," *Applied Catalysis A: General*, vol. 298, pp. 109-114, 2006.
[15] A. Naydenov, D. Mehandjiev, "Complete oxidation of benzene on manganese dioxide by ozone," *Applied Catalysis A: General*, vol. 97, № 1, pp. 17-22, 1993.
[16] Palcevskis E, Kulikova L, Serga V, Cvetkov A, Čornaja S, Sproge E and Dubencovs K, "Catalyst materials based on plasma-processed alumina nanopowder," *Journal of the Serbian Chemical Society*, vol. 77, № 12, pp. 1799-1806, 2012.
[17] Serga V, Kulikova L, Cvetkov A and Krumina A, "EPM Fine-Disperse Platinum Coating on Powder Carriers," *IOP Conf. Ser.: Mater. Sci. Eng*., vol. 38, 012062, 2012.
[18] Goeppert, A., et al, "Nanostructured silica as a support for regenerable high-capacity organoamine-based CO_2 sorbents," *Energy Environ. Sci*., vol. 3, № 12, pp. 1949-1960, 2010.
[19] H. Einaga, N. Maeda, S. Yamamoto, Y. Teraoka, “Catalytic properties of copper-manganese mixed oxides supported on SiO_2 for benzene oxidation with ozone,” *Catal. Today*, vol. 245, pp. 22-27, 2015.
[20] Centers for Disease Control and Prevention (CDC). (Online) https://emergency.cdc.gov/agent/benzene/basics/facts.asp.
[21] Agency for Toxic Substances and Disease Registry, ATSDR’s Substance Priority List. (Online) https://www.atsdr.cdc.gov/spl/#2019spl.
[22] G. S. Issa, M. D. Dimitrov, D. G. Kovacheva, T. S. Tsoncheva, "Nanosized mesoporous titania composites promoted with ceria and zirconia as catalysts for ethyl acetate oxidation: effect of preparation procedure," *Bulgarian Chemical Communications*, Vol. 50, Special issue H, pp. 80-86, 2018.
[23] M. Piumetti, D. Fino, N. Russo, “Mesoporous manganese oxides prepared by solution combustion synthesis as catalysts for the total oxidation of VOCs,” *Applied Catalysis B: Environmental*, Vol. 163, pp. 277-287, 2015.